5-ALA/SFC Mitigates Tau Toxicity via Lowering Oxidative Stress in a *Drosophila* Model of Tau Toxicity

Arisa Tamura [†] , Marie Noguchi [†] , Naoko Nozawa , Emiko Suzuki , Kanae Ando [*]

Posted Date: 10 March 2026

doi: 10.20944/preprints202603.0731.v1

Keywords:

mitochondria 1; 5-ALA/SFC 2; *Drosophila* model of tauopathy 3; oxidative stress 4; neurodegeneration 5

 doi:10.20944/preprints202603.0731.v1

Article

5-ALA/SFC Mitigates Tau Toxicity via Lowering Oxidative Stress in a *Drosophila* Model of Tau Toxicity

Arisa Tamura [1,†], Marie Noguchi [1,†], Naoko Nozawa [2], Emiko Suzuki [1], and Kanae Ando [1,3,*]

[1] Department of Biological Sciences, Graduate School of Science, Tokyo Metropolitan University, Hachioji, Tokyo, 192-0397, Japan

[2] Division of Pharmaceutical Research, SBI Pharmaceuticals Co., Ltd., Tokyo, 106-6020, Japan

[3] Department of Biological Sciences, School of Science, Tokyo Metropolitan University, Hachioji, Tokyo, 192-0397, Japan

* Correspondence: k_ando@tmu.ac.jp

† These authors contributed equally.

Abstract

Mitochondrial dysfunctions are believed to contribute to the pathogenesis of tauopathies, a group of neurodegenerative diseases with abnormal accumulation of microtubule-associated protein tau. The combination of 5-aminolevulinic acid (5-ALA) and sodium ferrous citrate (SFC) is known to improve mitochondrial functions. Here, we report that 5-ALA combined with SFC (5-ALA/SFC) improves mitochondrial functions and mitigates neurodegeneration in transgenic *Drosophila* expressing human tau. We found that tau reduces ATP levels, decreases mitochondrial distribution to neurites, and increases mitochondrial reactive oxygen species (ROS). Expression of oxidative phosphorylation (OXPHOS) genes was upregulated and activities of complexes I and IV were elevated. Feeding 5-ALA/SFC to tau flies lowers oxidative damages without correcting OXPHOS activities or mitochondrial distribution. 5-ALA/SFC treatment suppressed pathological tau phosphorylation and mitigated tau-induced neurodegeneration. Our results suggest that 5-ALA/SFC decreases a neurodegenerative pathway involving tau, mitochondria, and ROS.

Keywords: mitochondria 1; 5-ALA/SFC 2; *Drosophila* model of tauopathy 3; oxidative stress 4; neurodegeneration 5

1. Introduction

As the world population ages, the number of people suffering from neurodegenerative diseases are rapidly increasing, posing significant challenges for healthcare systems and society as a whole [1]. Aging increases the risk of Alzheimer's disease (AD) and other neurodegenerative diseases [2]. Many of these disorders are pathologically characterized by the abnormal accumulation of the microtubule-associated protein tau, collectively called tauopathy [3]. Tau is a microtubule-associated protein with a highly flexible structure; however, in tauopathy brains, tau is hyperphosphorylated and aggregated [4–6]. Accumulation of abnormal tau causes neurodegeneration [7], while how tau causes neurodegeneration is not fully understood.

Mitochondria play critical roles in neuronal functions via providing most of the ATP required for brain neurons through electron transfer chain and oxidative phosphorylation (OXPHOS) [8,9]. During OXPHOS, complexes I, III, and IV pump protons into the intermembrane space, generating the mitochondrial membrane potential that drives complex V, the ATP synthase to produce ATP [10]. Electron leakage from the chain forms superoxide anions, which are subsequently converted into hydrogen peroxide (H_2O_2), hydroxyl radicals (•OH), and superoxide (O_2^-) [8]. These reactive oxygen

 doi:10.20944/preprints202603.0731.v1

species (ROS) are primarily produced at complexes I and III [8,11], which can cause oxidative damage. Mitochondria also serve as a Ca^{2+} sink to maintain Ca^{2+} homeostasis for neuronal activity [12]. Mitochondrial abnormalities are observed in the brains of patients suffering from AD and other neurodegenerative diseases, and boosting mitochondrial functions may delay or treat neurodegenerative conditions [8].

5-aminolevulinic acid (5-ALA) has emerged as a potential strategy to improve mitochondrial functions [13]. 5-ALA is a precursor of heme and synthesized from succinyl-CoA and glycine in mitochondria [14]. 5-ALA is crucial for mitochondrial functions, which relies on heme in the OXPHOS complexes II, III, IV, and cytochrome c [15]. A combination of 5-ALA and sodium ferrous citrate (SFC) (5-ALA/SFC) boost mitochondrial functions in cultured fibroblasts, *Drosophila*, and mice [16–20]. 5-ALA/SFC treatment protects against age-related functional declines and lethality caused by CI deficiency in *Drosophila* [20,21]. In a triple transgenic mouse model of AD (3x-Tg), 5-ALA/SFC feeding increased mitochondrial protein levels [22]. However, the effects of 5-ALA/SFC on tau toxicity remains unknown.

In this study, we investigated tau-induced changes in mitochondria and the effects of 5-ALA/SFC on them as well as tau toxicity. A *Drosophila* model of tau toxicity has been established by expressing human tau in neurons or eyes [23], which recapitulate key pathological features of tauopathy such as tau phosphorylation at disease-related sites and neurodegeneration [23–26]. With this model, we found that feeding 5-ALA/SFC reduced ROS and mitigates tau-induced neurodegeneration.

2. Materials and Methods

2.1. Fly Stocks

Transgenic fly lines carrying human 0N4R tau were a kind gift from Dr. Mel Feany (Harvard Medical School) [23]. The GMR-Gal4 (RRID: BDSC_1104) and elav-Gal4 (RRID: BDSC_458) driver lines were obtained from the Bloomington Drosophila Stock Center. Flies with UAS-mito-roGFP-Grx1 (RRID: BDSC_67664) were obtained from Bloomington Stock Center [27].

Drosophila was kept in a constant temperature chamber at 25 °C with a 12-hour cycle of light and dark conditions. Adult flies were transferred to fresh vials after eclosion and transferred to fresh food vials every 2 to 3 days. The genotypes of flies used in each experiment are listed in Table 1.

Table 1. Fly genotypes used in this study.

Figure 1	control	*elav-Gal4/Y;UAS-mito-roGFP2-Grx1^{9}/+;UAS-luciferase/+*
	tau	*elav-Gal4/Y;UAS-mito-roGFP2-Grx1^{9}/+;UAS-tau/+*
Figure 2	control	*elav-Gal4/Y;UAS-tdTomato/+;+/+*
	tau	*elav-Gal4/Y;+/+;UAS-tau/+*
Figure 3A	control	*elav-Gal4/Y;+/+;+/+*
	tau	*elav-Gal4/Y;+/+;UAS-tau/+*
Figure 3B	control	*elav-Gal4/Y;+/+;+/+*
	tau	*elav-Gal4/Y;UAS-tau/CyO;+/+*
Figure 3C	control	*elav-Gal4/Y;+/+;+/+*
	tau	*elav-Gal4/Y;+/+;UAS-tau/+*
Figure 3D	control	*+/+;gmr-Gal4/+;+/+*
	tau	*+/+;gmr-Gal4/+;UAS-tau/+*
Figure 4	tau −	*elav-Gal4/Y;+/+;+/+*
	tau +	*elav-Gal4/Y;+/+;UAS-tau/+*

 doi:10.20944/preprints202603.0731.v1

Figure 5	tau −	*elav-Gal4/Y;+/+;+/+* *+/Y;gmr-Gal4/+;+/+*
	tau +	*elav-Gal4/Y;+/+;UAS-tau/+* *+/Y;gmr-Gal4/+;UAS-tau/+*
Figure 6A	tau −	*+/+;gmr-Gal4/+;+/+*
	tau +	*+/+;gmr-Gal4/+;UAS-tau/+*
Figure 6B	tau −	*+/+;gmr-Gal4/+;+/+*
	tau +	*+/+;gmr-Gal4/+;UAS-tau/+*
Figure 6C		*+/+;gmr-Gal4/+;UAS-tau/+*
Figure 7		*+/+;gmr-Gal4/+;UAS-tau/+*
Figure 8		*+/+;gmr-Gal4/+;UAS-tau/+*

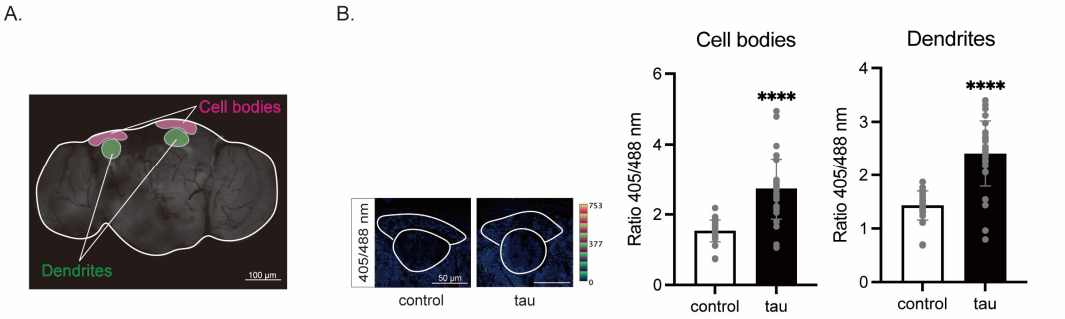

Figure 1. Relative oxidation levels of mitochondrial glutathione redox potential biosensor mito-roGFP2-Grx1 expressed in neurons with or without co-expression of tau. Male flies at 3 days after eclosion were used. **(A)** Schematic representation of cell body region and dendritic region in the mushroom body of the fly brain. **(B)** Representative ratiometric images of mito-roGFP2-Grx1 (left), and quantitation of oxidized/reduced roGFP (right). Data are expressed as mean ± SE, n = 29; ****p < 0.0001; Student's t-test.

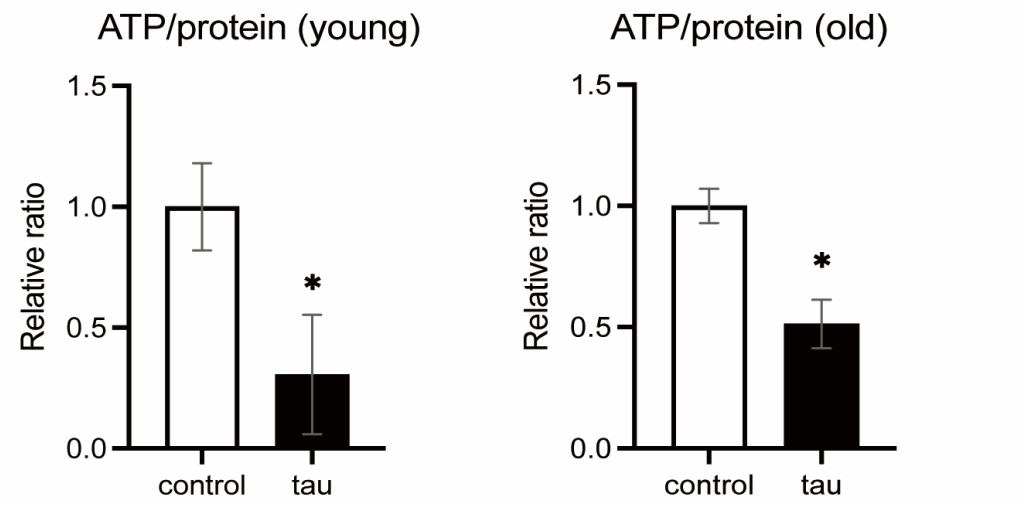

Figure 2. 10 heads of male flies expressing tau in neurons at 2 days after eclosion (left, young) and 46-49 days after eclosion (right, old) were homogenized and subjected to ATP assay. ATP levels were normalized by protein levels and expressed as relative ratio. Data are expressed as mean ± SE, n = 3; *$p < 0.05$; Student's t-test.

 doi:10.20944/preprints202603.0731.v1

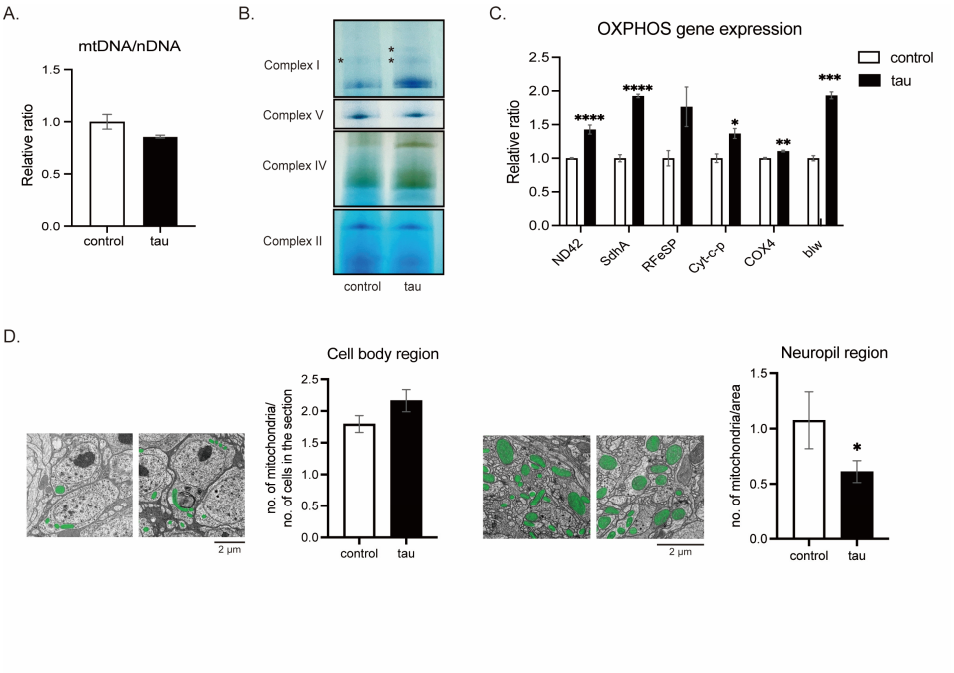

Figure 3. (A) Levels of mtDNA and nDNA in heads of male flies with neuronal tau expression were assessed by qRT-PCR, and the ratio of mtDNA to nDNA are shown as relative ratio. Flies were 1-2 days after eclosion. Data are expressed as mean ± SE, n = 3; $p > 0.05$; Student's t-test. **(B)** Tau expression increases complexes I and IV activities. Mitochondria were extracted from 120 heads of flies with neuronal tau expression and subjected to Blue Native PAGE followed by In-gel activity assay to assess the activities of OXPHOS complexes I, II, IV, and V. Flies were 0-3 days after eclosion. Asterisk denotes supercomplex. **(C)** Tau expression upregulates expression of genes coding OXPHOS components. Extracts of heads with neuronal tau expression were subjected to qRT-PCR. Flies were 10 days after eclosion. Data are expressed as mean ± SE, n = 3; *$p < 0.05$, **$p < 0.01$, ***$p < 0.005$, ****$p < 0.0001$; Student's t-test. **(D)** Tau reduces mitochondrial distribution to the neurite. Electron microscopic analysis of mitochondria in the brain of the flies expressing tau in neurons at 50 day-old. The number of mitochondria (colored green) in the cell body region per the number of cells (left) and that of neuropil region per area of observation (right) were analyzed. Representative images and quantitative analysis are shown. Data are expressed as mean ± SE, n = 3-12; *$p < 0.05$; one-way ANOVA followed by Dunnett's test.

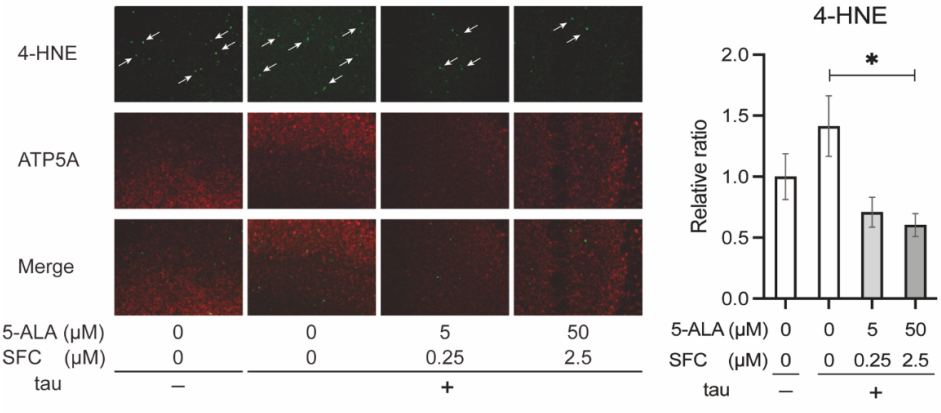

Figure 4. Immunostaining of the brains of driver-only control or flies with neuronal tau expression fed with 5-ALA and SFC at the indicated concentration with antibodies against a marker of lipid peroxidation, 4-HNE (green, arrows), and mitochondrial marker, ATP5A (red). Representative images and quantitative analysis are shown. Data are expressed as mean ± SE, n = 6-8; *$p < 0.05$; one-way ANOVA followed by Dunnett's test.

 doi:10.20944/preprints202603.0731.v1

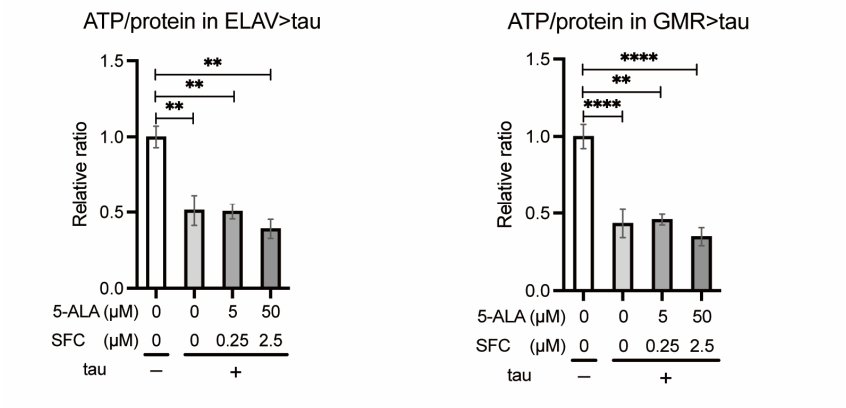

Figure 5. ATP levels in the heads of flies with tau expression in neurons at 46 to 49 days after eclosion (left) or those in the eye at 10 days-old (right) normalized with protein levels indicated as relative ratio to the control. Data are expressed as mean ± SE, n = 3; $^{**}p < 0.01$, $^{****}p < 0.0001$; one-way ANOVA followed by Dunnett's test.

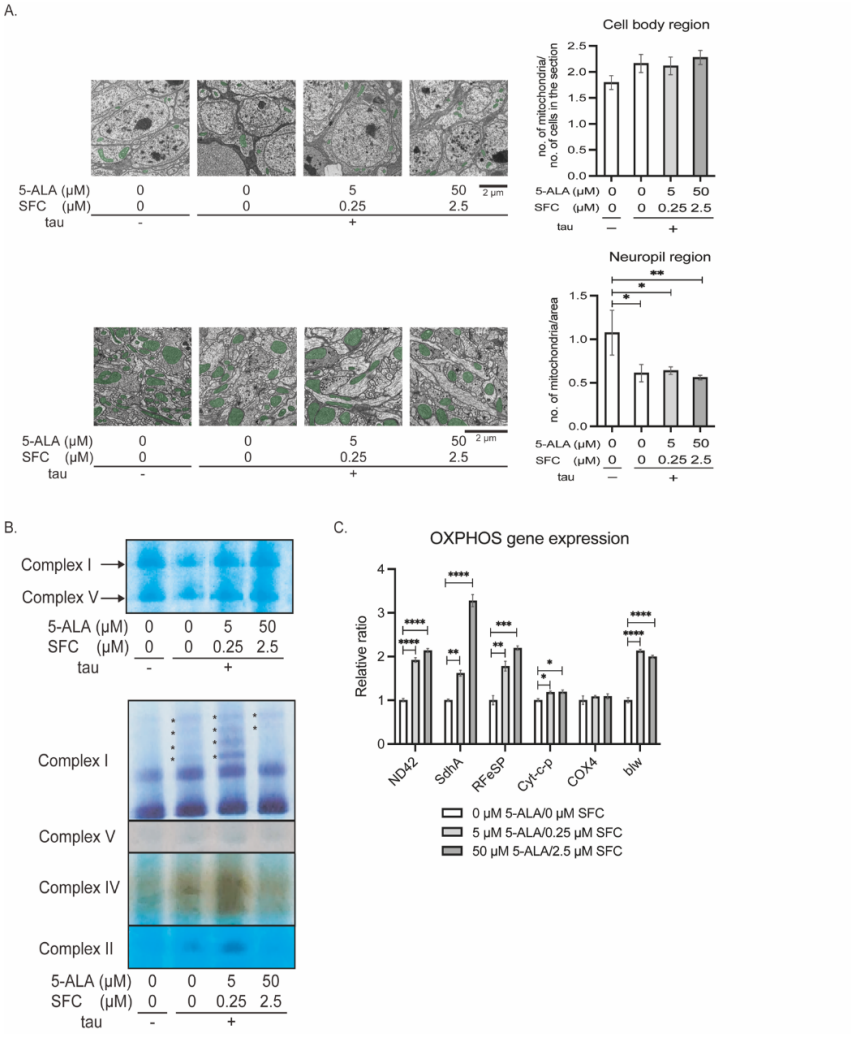

Figure 6. (A) Ultrastructural analysis of heads of flies at 48 to 50 days after eclosion. The number of mitochondria (green) in the cell body region per the number of cells (top), that of neuropil region per area of observation (bottom) were analyzed. Representative images (left) and quantitative analysis (right). Data are expressed as mean ± SE, n = 3-12; $^{*}p < 0.05$, $^{**}p < 0.01$; one-way ANOVA followed by Dunnett's test. Data for flies without tau

 doi:10.20944/preprints202603.0731.v1

expression and those with tau expression without 5-ALA/SFC are the same as those shown in Figure 3D. **(B)** Mitochondria were extracted from 120 heads of tau flies and subjected to high-resolution Clear Native PAGE (top) and IGA (bottom). **(C)** Head extracts were subjected to qRT-PCR. Flies were at 10 days after eclosion. Data are expressed as mean ± SE, n = 3; *$p < 0.05$, **$p < 0.01$, ***$p < 0.005$, ****$p < 0.0001$; Student's t-test.

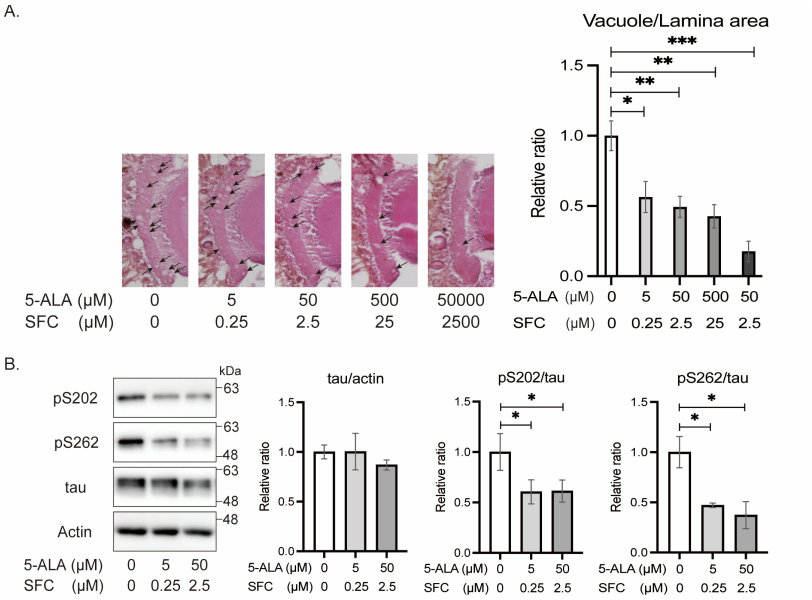

Figure 7. (A) Tau-induced neurodegeneration is observed as vacuoles in the lamina (arrows). Representative images (left) and quantitation of vacuole are divided by the area of lamina are shown (right). Flies were 10 day-old. Data are expressed as mean ± SE, n = 5; *$p < 0.05$, **$p < 0.01$, ***$p < 0.001$; one-way ANOVA followed by Dunnett's test. **(B)** Western blotting of head lysate with tau and phospho-tau specific antibodies. Actin was used as a loading control. Representative blots (left) and quantitative analysis (right). Data are expressed as mean ± SE, n = 3-4; *p < 0.05; one-way ANOVA followed by Dunnett's test.

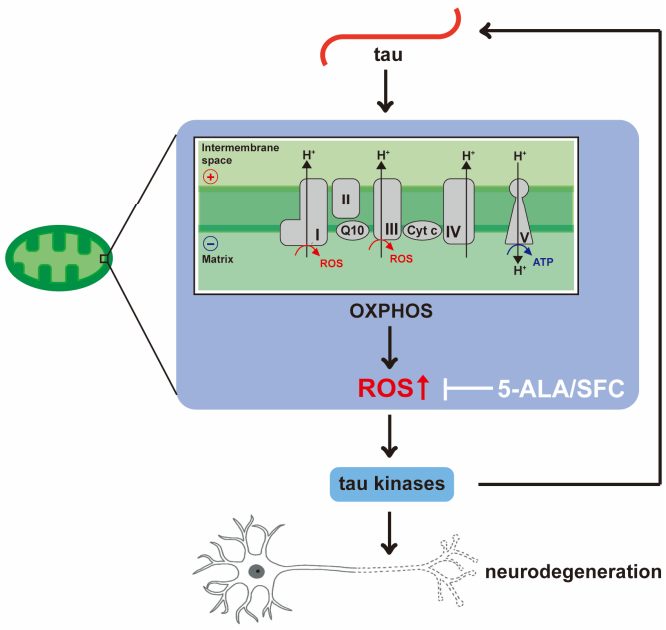

Figure 8. A model of feed-forward mechanism consists of mitochondria, ROS and tau phosphorylation. Tau disrupts OXPHOS and increases mitochondrial ROS levels. Elevated ROS activates tau kinases, enhancing tau

 doi:10.20944/preprints202603.0731.v1

phosphorylation and further disrupting mitochondrial function. 5-ALA/SFC attenuates this feed-forward cascade by reducing ROS.

2.2. 5-ALA/SFC Feeding

Flies were raised on cornmeal food without 5-ALA (hydrochloride)/SFC or with the indicated concentrations of 5-ALA (hydrochloride)/SFC at 25 °C under 12 h light-12 h dark cycles. Flies were transferred to fresh vials every 2 to 3 days.

2.3. ROS Analysis with Mito-roGFP2-Grx1

Flies were anesthetized with CO_2, and brains were dissected in PBS-NEM (137mM NaCl, 2.7mM KCl, 10mM Na_2HPO_4, 1.8 mM KH_2PO_4, 20 mM NEM, pH 7.4). The brains were incubated for 5 min in PBS-NEM at room temperature and then fixed for 8 min in 4% PFA/PBS-NEM. Brains were washed with PBS-NEM three times, imaged on the same day through a laser confocal microscope (Nikon C2, Nikon, Tokyo, Japan), and analyzed with ImageJ [28]. Flies used for this assay were 3 days old after eclosion.

2.4. ATP Assay

ATP was extracted as previously described [29] using 6 M guanidine-HCl in extraction buffer (100 mM Tris and 4 mM EDTA, pH 7.8) and ATP Determination Kit (Cat#: A22066, Invitrogen, Carlsbad, California, USA). Luminescence was measured on an EnSpire Multimode Plate Reader (PerkinElmer, CT, USA). Relative ATP levels were determined by normalizing luminescence values to total protein concentrations, using the Bradford method. Flies used for ATP assay were 10 days old (GMR>tau), 0 to 1 day old, and 46 to 49 days (elav>tau) after eclosion.

2.5. Mitochondrial DNA (mtDNA)/Nuclear DNA (nDNA) Ratio

mtDNA extraction for mitochondrial quantification was performed following a modified protocol [21]. Total DNA was purified from 60 fly heads using QIAamp DNA Mini Kit (Cat#: 51304, QIAGEN, Venlo, Netherlands). The expression levels of target genes were measured using THUNDERBIRD SYBR qPCR Mix (Cat#: QPS-201, TOYOBO, Osaka, Japan)on a Thermal Cycle Dice TP800 (Takara Bio, Shiga, Japan). For mtDNA quantification, the average expression levels of *mt:COI*, *mt:COIII*, and *mt:CytB* were used. nDNA was quantified using the mean expression levels of *Sicily*, *Act5C*, and *rp49*. Analysis of mtDNA/nDNA ratio was calculated by following the △△Ct method used for RT-qPCR analysis [30]. Flies used for mtDNA analysis were 1-2 days old after eclosion. Primer sequences (5′-3′) were as follows: *mt:COI* (F, AAAGTTGACGGTACACCTGG) (R, AGGAACACTTTCAATTACAATCGG), *mt:COIII* (F, CACGAGAAGGAACATACC) (R, GCGGGTGATAAACTTCTG), *mt:CytB* (F, GAAAATTCCGAGGGATTCAA) (R, AACTGGTCGAGCTCCAATTC), *Sicily* (F, AGTGGAGAAATACGACTACGAGA) (R, GATGGCCGCTAACCGATCTG), *Act5C* (F, AAGCTGTGCTATGTTGCCCT) (R, ATTCCCAAGAACGAGGGCTG), and *rp49* (F, ATCGTGAAGAAGCGCACCAA) (R, GTCGATACCCTTGGGCTTGC).

2.6. Blue Native PAGE (BN-PAGE)

BN-PAGE to analyze mitochondrial respiratory chain protein was carried out as described with a modification [31,32]. Heads from 120 flies were homogenized in 1 ml of chilled mitochondrial isolation medium (250 mM sucrose, 10 mM Tris-HCl (pH 7.4), 0.15 mM $MgCl_2$). The samples were centrifuged twice for 15 min at 600 g at 4 °C to remove debris. The supernatant was centrifuged again for 5 min at 13,000 g at 4 °C to collect mitochondrial fraction as the pellet. Mitochondrial protein levels were determined by bicinchoninic acid (BCA) assay (Cat#:126625-50ML, Sigma, Kanagawa, Japan). For BN-PAGE, The NativePAGE Novex Bis-Tris Gel System (Cat#:BN1001BOX, Life Technologies, CA, USA) was used according to the manufacturer's protocol. 17-96 μg mitochondrial protein were

 doi:10.20944/preprints202603.0731.v1

solubilized in sample buffer (50 mM NaCl, 20 mM Tris-HCl (pH 7.4), 1% Triton-X100). After centrifugation for 5 min at 14,000 rpm at 4 °C, the supernatants were collected and mixed with 10x loading dye solution (5% Coomassie Blue G, 1M aminohexanoic acid, 100 mM Bis-Tris) and separated on 3-12% NativePAGE gels.

2.7. In-Gel Activity Assay (IGA)

IGA to analyze mitochondrial respiratory chain activity was carried out as described previously with a modification [33]. Mitochondrial fractions were subjected to BN-PAGE. For complex I activity, the gel was incubated in complex I activity substrate (2 mM Tris-HCl (pH 7.4), 0.01% (w/v) NADH, 0.025% (w/v) Nitrotetorazolium Bule chloride (NTB)) for 15 min at room temperature. The gel was then transferred to 10% acetic acid to stop the reaction. For complex II activity, the gel was incubated in complex II activity substrate (5 mM Tris-HCl (pH 7.4), 20 mM Sodium Succinate, 0.025% (w/v) NTB, 200 μM Phenazine Methosulphate) for 40 min at 37 °C. The gel was then transferred to 10% acetic acid to stop the reaction. For complex IV activity, the gel was incubated with complex IV activity substrate (0.05% (w/v) Diaminobenzidine (DAB), 0.01% (w/v) cytochrome c, 45 mM phosphate buffer (pH 7.4)) overnight at room temperature. For complex V activity, the gel was incubated with CV activity substrate (35 mM Tris, 270 mM glycine, 14 mM $MgSO_4$, 10 mM ATP, 0.2% (w/v) $Pb(NO_3)_2$) overnight at room temperature. The gel was transferred to 50% of methanol to stop the reaction. Flies used for IGA were 2-3 days old after eclosion.

2.8. Quantitative Reverse Transcription PCR (qRT-PCR)

30 flies were collected and frozen with liquid nitrogen. Heads were homogenized, and total RNA was extracted in ISOGEN(Cat#:311-02501, Nippon Gene, Tokyo, Japan). The concentration and purity of the total RNA were measured with NanoDrop One Spectrophotometer (Thermo Scientific, Waltham, MA, USA). 500 ng of total RNA was subjected to cDNA synthesis using ReverTra Ace qPCR RT Master Mix with gDNA Remover. Quantitative real-time PCR was performed using THUNDERBIRD SYBR qPCR Mix on a Thermal Cycler Dice TP800 (Takara Bio, Shiga, Japan). The expression level of each gene was normalized either to the expression level of Actin or rp49. Flies used for RT-qPCR were 10 days old after eclosion. Primer sequences (5′-3′) were as follows: *Actin* (F, TGCACCGCAAGTGCTTCTAA) (R, TGCTGCACACTCCAAACTTCCA), *rp49* (F, ATCGTGAAGAAGCGCACCAA) (R, GTCGATACCCTTGGGCTTGC), *ND42* (F, ACACAGTCGCCCAATCTACTC) (R, GCTGTACTTCTTCGTCTTGTACG), *SdhA* (F, TGTACGACACGGTCAAGGG) (R, TTCTCCAGCTCAATGACAGCC), *RFeSP* (F, GTCCTCTCCACGGGATTGAA) (R, TGAAGGTGTTAACCAGGCCC), Cyt-c-p (F, AAGCACAAGGTTGGACCCAA) (R, AAGATCATCTTGGTGCCGGG), *COX4* (F, TACGATGAGCTGCCCGTTAC) (R, GGTTGATTTCCAGGTCGATGAT), and *blw* (F, CCGTTTCCGTGTGGGAATCAA) (R, AGAGCGGTCTTACCAGTCTGA).

2.9. Electron Microscopy

Flies were anesthetized with CO_2, and their heads were cut into halves in primary fixative solution (2% PFA and 2.5% in 0.1 M Na cacodylate buffer). The heads were incubated in the fixative solution for 2 h at room temperature and then overnight at 4 °C. The samples were washed with 3% sucrose in 0.1 M Na cacodylate buffer three times for 5 min each on ice. The samples were then incubated in ice-cold secondary fixative solution (1% OsO4 in 0.1 M Na cacodylate buffer) for 1 h on ice and washed with H_2O three times for 5 min on ice. After washing, samples were dehydrated with ethanol and embedded in an Epon mixture (Cat#:3402, NEM, Tokyo, Japan). 50 nm of ultra-thin sections were sliced sagittally and collected on copper grids. The sections were stained with 2% uranyl acetate in 70% ethanol and Reynolds' lead citrate solution. Images were captured under a transmission electron microscope JEM-1400Plus (JEOL Ltd., Tokyo, Japan) and analyzed manually. Flies used for electron microscopic analysis were 48 to 50 days old after eclosion.

 doi:10.20944/preprints202603.0731.v1

2.10. Anti-4-Hydroxynonenal (4-HNE) Staining

Flies were anesthetized with CO_2, and brains were dissected in cold Schneider's Drosophila Medium (Cat#:21720024, Thermo Fisher Scientific, Waltham, MA, USA). The brains were fixed with 4% PFA for 40 min at room temperature and then washed with 0.1% PBST (0.1% Triton in PBS) three times for 5 min. Then, the samples were blocked with 1% NGS in 0.1% PBST for 1 h at room temperature. After blocking, the samples were incubated with anti-4-HNE antibody (Cat#:46545, Abcam, Cambridge, UK) (1:100) in 1% normal goat serum (Cat#:551-76253, FUJIFILM, Tokyo, Japan) in 0.1% PBST at 4 °C overnight. The next day, the samples were washed with 0.1% PBST three times for 5 min, then incubated with Alexa-Flour 647-conjugated anti-rabbit IgG (1:500) for 3 h at room temperature. The samples were again washed with 0.1% PBST three times for 5 min and mounted. Images were captured under a laser confocal microscope Zeiss LSM 710 (Zeiss, Oberkochen, Germany) and analyzed with ImageJ [28]. Flies used for this assay were 48 to 50 days old after eclosion.

2.11. High-Resolution Clear Native PAGE (hrCNE)

hrCNE to analyze mitochondrial respiratory chain protein was carried out as described with a modification [21]. Heads from 120 flies were homogenized in 1 ml of chilled mitochondrial isolation medium (250 mM sucrose, 10 mM Tris-HCl (pH 7.4), 0.15 mM $MgCl_2$). The samples were centrifuged twice for 15 min at 600 g at 4 °C to remove debris. The supernatant was centrifuged again for 5 min at 13,000 g at 4 °C to collect mitochondria as a pellet. Mitochondrial protein levels were determined by BCA assay(Cat#:126625-50ML, Sigma, Kanagawa, Japan). Mitochondrial fractions were incubated in sample buffer (50 mM NaCl, 50 mM imidazole/HCl, 2 mM 6-aminohexanoic acid, 1 mM EDTA (pH 7.0), DDM (2.5 g/g protein), Digitonin (4 g/g protein)) for 10 min on ice. After centrifugation for 15 min at 10,000 g at 4 °C, the supernatants were mixed with 10x loading dye solution (50% glycerol, 0.1% Ponceau S) and separated on 3-12% NativePAGE Novex Bis-Tris Gel System (Cat#:BN1001BOX, Life Technologies, CA, USA). The gels were stained with a colloidal blue staining kit (Thermo Fisher Scientific, Waltham, MA, USA).

2.12. Histological Analysis

Fly heads were dissected and fixed in Bouin's fixative solution for 48 h at room temperature. The heads were washed three times with 50 mM Tris/150 mM NaCl and incubated overnight at room temperature. Then, the samples were dehydrated with ethanol and subjected to paraffin embeddings. 7 μm of serial sections were sliced and stained with hematoxylin and eosin. Images were captured under a bright field of Keyence microscope BZ-X700 (Keyence, Osaka, Japan), and the area of vacuoles was analyzed with ImageJ [28]. Flies used for vacuole formation in lamina were 10 days old after eclosion.

2.13. Western Blotting

Fifteen flies were collected and frozen with liquid nitrogen. Heads were homogenized in SDS-Tris-Glycine sample buffer, and the lysate was loaded to the lanes of a 10% Tris-Glycine gel. The gel was then transferred to the PVDF membrane (Cat#:IPVH00010, Merck Millipore, MO, USA), and the membrane was blocked with 5% skim milk (Morinaga, Tokyo, Japan) for 1 h at room temperature. The membrane was incubated with antibodies in 5% skim milk and then visualized using Immobilon Western Chemiluminescent HRP Substrate (Cat#:WBKLS0050, Merch Millipore, MO, USA). Images were captured under the Fusion FX (Vilber, Marne-la-Vallée, France), and band intensity was analyzed with ImageJ [28]. Flies used for Western blotting were 10 days old after eclosion. Anti-tau (T46, Cat#:13–6400, Thermo Fisher Scientific, Waltham, MA, USA), anti-pSer202, anti-pSer262 (pSer262, Cat#:ab92627, Abcam, Cambridge, UK), anti-actin (Cat#:A2066, Sigma, Kanagawa, Japan) were purchased. Anti-pSer202 (CP13) was a kind gift from Dr. Peter Davis (Albert Einstein College of Medicine).

 doi:10.20944/preprints202603.0731.v1

2.14. Statistical Analysis

The number of replicates, what n represents, precision measurements, and the meaning of error bars are indicated in Figure Legends. For pairwise comparisons, Student's t-test was performed with Microsoft Excel (Microsoft). For multiple comparisons, data were analyzed using one-way ANOVA with post-hoc test in the GraphPad Prism 6.0 software (GraphPad Software, Inc., La Jolla, CA). Results with a p-value of less than 0.05 were considered to be statistically significant.

3. Results

3.1. Effects of Tau on Mitochondria

3.1.1. Tau Increases Mitochondrial ROS in Neurons

We set out to characterize tau-induced changes in mitochondria in neurons. First, we analyzed ROS levels in tau-expressing neurons in the fly brain by using a mitochondrial redox sensor specific to the glutathione reducing pool, mito-roGFP2-Grx1 [27]. The redox-sensitive green fluorescent proteins (roGFPs) contain an oxidizable dithiol pair on their surface, and after oxidation-induced disulfide bond formation, mito-roGFP2-Grx1 converts from 488 nm to UV excitation [34]. mito-roGFP2-Grx1 [27] was co-expressed with human tau in neurons using the pan-neuronal driver, *elav-Gal4*, and signals in the mushroom body, where the cell body region and dendritic region are easily located, were quantified (Figure 1A). We found that tau expression causes higher oxidation, both in the dendrites and cell bodies of the mushroom body (Figure 1B), indicating that tau expression enhances mitochondrial ROS production.

3.1.2. Tau Expression Reduces ATP Levels

Next, we analyzed ATP levels in the heads of flies with or without tau expression in neurons at young age (2 days after eclosion) and old age (46-49 days after eclosion). ATP levels were significantly reduced in tau-expressing flies compared to controls, in both young and aged cohorts (Figure 2).

3.1.3. Tau Does Not Reduce the Number of Mitochondria

To determine whether ATP reduction is caused by lower mitochondrial number, mtDNA levels were analyzed. Tau expression did not alter the relative mtDNA levels (Figure 3A), indicating that a reduction in ATP levels (Figure 2) is not due to loss of mitochondria.

A decrease in ATP levels and an increase in ROS levels may be due to defects in OXPHOS. We examined the activities of OXPHOS complexes in the heads of flies with or without neuronal expression of tau. Blue Native-PAGE (BN-PAGE) followed by In-gel activity assay (IGA) revealed that tau increases the activities of complexes I and IV (Figure 3B). We also noticed that tau increased supercomplexes containing complex I (Figure 3B, asterisk). The activities of complexes II and V were similar between control and tau (Figure 3B). qRT-PCR revealed that neuronal expression of tau increases expression of mRNA coding proteins in the OXPHOS complexes and cytochrome c (Figure 3C).

We also analyzed the morphology and distribution of mitochondria in the cell body region (Figure 3D, left) and neuropil region (Figure 3D, right) under a transmission electron microscope. The number of mitochondria in the neuropil region was lower in the tau-expressing fly brain (Figure 3D, right) but similar in the cell body region to that of the control (Figure 3D, left). Abnormality in mitochondrial morphology was not detected.

These results suggest that tau expression promotes the activity of OXPHOS complexes I and IV, which is consistent with higher ROS levels.

 doi:10.20944/preprints202603.0731.v1

3.2. Effects of 5-ALA/SFC Feeding on Tau Toxicity

3.2.1. 5-ALA/SFC Reduces Oxidative Damage Caused by Tau

We analyzed the effect of 5-ALA/SFC feeding on oxidative stress induced by tau. The brains of the flies expressing tau in neurons at 48 days after eclosion were stained with anti-4-HNE antibody to detect lipid peroxidation and ATP5A to detect mitochondria [35]. Tau expression increased 4-HNE signals, while 5-ALA/SFC feeding reduced them (Figure 4), indicating that 5-ALA/SFC feeding lowers oxidative stress caused by tau.

3.2.2. 5-ALA/SFC Does Not Increase ATP Levels in Tau Flies

We analyzed the effects of 5-ALA/SFC on ATP levels reduced by tau expression. ATP assay of head extracts of the flies expressing tau in neurons (ELAV>tau) or in the eyes (GMR>tau) revealed 5-ALA/SFC feeding did not increase ATP levels (Figure 5).

3.2.3. 5-ALA/SFC Does Not Correct Mitochondrial Distribution and OXPHOS Activities in Tau Flies

We analyzed the effects of 5-ALA/SFC on mitochondrial distribution and morphology in the brain. 5-ALA/SFC treatment did not affect the number of mitochondria in the cell body region (Figure 6A, top). Tau expression reduced mitochondrial number in the neuropil region, and 5-ALA/SFC treatment further reduced it, in the neuropil region (Figure 6A, bottom).

We assessed the amount and activities of OXPHOS complexes by high-resolution Clear Native PAGE (hrCNE) and IGA. hrCNE revealed that the protein levels of complexes I and V were similar with or without 5-ALA/SFC feeding (Figure 6B, top). IGA showed that the elevated activities of complexes I, II, and IV in tau flies were further increased by 5-ALA/SFC feeding (Figure 6B, bottom). Also, expression of OXPHOS protein-coding genes in tau flies were further increased with 5-ALA/SFC feeding (Figure 6C).

3.2.4. 5-ALA/SFC Reduces Tau Phosphorylation at Disease-Associated Sites and Mitigates Tau-Induced Neurodegeneration

We analyzed the effects of 5-ALA/SFC on tau-induced neurodegeneration. Expression of tau in the retina causes degeneration of photoreceptor neurons, which is observed as vacuoles in lamina, the first optic neuropils [36]. We found that 5-ALA/SFC feeding suppressed tau-induced neurodegeneration in a dose-dependent manner (Figure 7A).

We asked whether 5-ALA/SFC affects tau protein levels and tau phosphorylation at disease-associated sites. Western blotting of head lysates with a tau antibody or with phospho-tau specific antibodies showed that 5-ALA/SFC feeding does not affect tau levels, while tau phosphorylation at Ser202 and Ser262 was significantly reduced with 5-ALA/SFC feeding (Figure 7B).

4. Discussion

In this study, we examined the effects of tau on mitochondrial functions in neurons and tested the effects of 5-ALA/SFC using transgenic *Drosophila*. We found that 5-ALA/SFC lowered oxidative damages, reduces tau phosphorylation and mitigates neurodegeneration. Our results suggest that 5-ALA/SFC protects neurons against tau toxicity.

4.1. Tau Directly Modifies OXPHOS Complexes

We found that tau expression increases mito-roGFP2-Grx1 signal, indicating that mitochondrial ROS production is increased (Figure 1). Since mitochondrial ROS is primarily generated by complex I activity [8,11], elevated mitochondrial ROS is likely to be caused by enhanced complex I activity induced by tau expression (Figure 3). Tau-expressing flies exhibited decreased brain ATP (Figure 2), suggesting that enhanced activities of complexes I and IV and elevated OXPHOS gene expression in these fly brains (Figure 3) may be a compensatory response to reduced ATP.

 doi:10.20944/preprints202603.0731.v1

Tau is known as a microtubule-associated protein, while its functions in mitochondria has been reported [37]. Comprehensive interactome analysis revealed that direct interactions between tau and proteins located on outer membrane of mitochondria such as transporters, those on inner membrane of mitochondria including OXPHOS components and regulators, and enzymes in the matrix [38]. Tau interacts with complex I components such as NDUFS1, and NDUFS3, complex III components such as Cytochrome c1, SDHB, UQCRC1, and UQCRC2, complex IV components such as COX4I1, COX5A, COX5B, COX7A2, complex V components such as ATP5A1, ATP5B, ATP5C1, ATO5F1, ATP5H, ATP5J, ATP5J2, ATP5O, ATP6V1E1, ATP5EP2, and OXPHOS regulator C1QBP and ATPIF1, and tau with pathological mutations show less interaction to some of these proteins [38]. Excess tau proteins may dysregulate functions of these complexes. Tau proteins also interact with enzymes critical for TCA cycle and amino acid metabolism such as malate dehydrogenase, fumarate hydratase, glutamate dehydrogenase 1, aspartate aminotransferase [38]. Thus, even with upregulation of OXPHOS complexes (Figure 3), dysregulation of these pathways can impair ATP synthesis. Tau interaction with mitochondrial anti-oxidant enzymes such as mitochondrial peroxiredoxin have been reported [38]. Although it is not clear how tau regulate their activity, excess tau may impair their functions and contribute to an increase in mitochondrial ROS.

4.2. 5-ALA/SFC Reduces Oxidative Damage

Elevated oxidative stress in tau flies was reduced by 5-ALA/SFC feeding (Figure 4). How does 5-ALA/SFC reduce oxidative damage? 5-ALA/SFC increased activities of complexes I, II, and IV (Figure 6B) and further increased OXPHOS transcripts in tau flies (Figure 6C). We also noticed that 5-ALA/SFC increased supercomplexes with complex I activity (Figure 6B). Supercomplex have been proposed to contribute to efficient electron transfer with less ROS production [39–41], thus 5-ALA/SFC may mitigate oxidative damages via promoting supercomplex formation. 5-ALA/SFC has been also reported to bypass mitochondrial complex I deficiency, by enhancing alternative electron entry to OXPHOS from complex II [21]. 5-ALA/SFC may shift metabolic programs to cope with imbalance of OXPHOS, and electron leak induced by tau.

4.3. 5-ALA/SFC Attenuates Tau Phosphorylation and Toxicity

We found that 5-ALA/SFC suppresses tau-induced neurodegeneration (Figure 7A). ROS increases cellular vulnerability to tau [42], thus, 5-ALA/SFC protects neurons by interaction with tau-induced cell death pathways. 5-ALA/SFC lowers tau phosphorylation at disease-associated sites (Figure 7B). Since tau phosphorylation at these sites, especially Ser262, is known to enhance tau-induced neurodegeneration [6,25,43,44], our results suggest that 5-ALA/SFC suppresses neurodegeneration via lowering neurotoxic tau species. ROS activate stress-induced kinases, such as MAPK, JNK, and GSK3β, which phosphorylate tau at Ser and Thr followed by proline including Ser202 [45]. Ser262, in a KXGS motif in a microtubule binding repeat, is not followed by proline [46], and not phosphorylated by these proline-directed kinases [46,47]. Instead, Ser262 is phosphorylated by AMPK family members [25,48]. Mitochondrial ROS has been reported to activate AMPK [48], and 5-ALA/SFC may lower AMPK activity via reduction of ROS in tau flies. Ser262 is also phosphorylated by Checkpoint kinase 2 (Chk2), which is activated by DNA damages [25]. ROS-induced DNA damage, and flowing activation of Chk2, may be lowered by 5-ALA/SFC. Our results suggest that tau, mitochondria and ROS forms a feed-forward mechanism leading to neurodegeneration, and 5-ALA/SFC mitigates this mechanism via decreasing ROS (Figure 8).

5. Conclusions

Our study revealed the functional interaction between tau and mitochondrial OXPHOS complex and protective effects of 5-ALA/SFC in vivo. Our results suggest that 5-ALA/SFC protects against tau toxicity via lowering ROS and tau phosphorylation. Further investigation in these pathways will

 doi:10.20944/preprints202603.0731.v1

advance our understanding of tau toxicity and mechanisms of the neuroprotective action of 5-ALA/SFC.

Author Contributions: Conceptualization, A.T., M.N., and K.A.; methodology, A.T., M.N., N.N., E.S., and K.A.; validation, A.T. and M.N.; formal analysis, A.T. and M.N.; investigation, A.T., M.N., and N.N.; writing—original draft preparation, A.T., M.N., and K.A.; writing—review and editing, A.T., M.N., and K.A.; visualization, A.T. and M.N.; supervision, K.A.; project administration, K.A.; funding acquisition, A.T. and K.A. All authors have read and agreed to the published version of the manuscript.

Funding: This research was supported by AMED under Grant Number JP24wm0625509 (K.A.), JP25wm0625509 (K.A.), Grant-in-Aid for Scientific Research (B) [24K02860] (K.A.), and MIYAKO-MIRAI Project of Tokyo Metropolitan University (A.T.).

Institutional Review Board Statement: The study was approved by the Institutional Review Board of Tokyo Metropolitan University (G5-15, G6-15, and G7-35).

Informed Consent Statement: Not applicable.

Data Availability Statement: The datasets used in this study are available from the corresponding author upon request.

Acknowledgments: Authors thank Drs Shin-ichi Hisanaga, Taro Saito, and Akiko Asada for insightful discussion. Authors thank Drs. Mel Feany and Peter Davis for *Drosophila* stocks and antibody. Stocks obtained from the Bloomington Drosophila Stock Center (NIH P40OD018537) were used in this study.

Conflicts of Interest: N.N. is employee of SBI Pharmaceuticals Co., Ltd. SBI Pharmaceuticals Co., Ltd. supplied 5-ALA/SFC, which had no role in the design of the study. The funders had no role in the design of the study; in the collection, analyses, or interpretation of data; in the writing of the manuscript; or in the decision to publish the results.

References

1. "2025 Alzheimer's disease facts and figures," *Alzheimers Dement.*, Apr. 2025, doi: 10.1002/alz.70235.
2. A. Eckert, K. Schmitt, and J. Götz, "Mitochondrial dysfunction - the beginning of the end in Alzheimer's disease? Separate and synergistic modes of tau and amyloid-β toxicity," *Alzheimers Res. Ther.*, vol. 3, no. 2, p. 15, May 2011, doi: 10.1186/alzrt74.
3. K. Iqbal, F. Liu, C.-X. Gong, and I. Grundke-Iqbal, "Tau in Alzheimer Disease and Related Tauopathies," *Curr. Alzheimer Res.*, vol. 7, no. 8, pp. 656–664, Dec. 2010, doi: 10.2174/156720510793611592.
4. S. Wegmann, J. Biernat, and E. Mandelkow, "A current view on Tau protein phosphorylation in Alzheimer's disease," *Curr. Opin. Neurobiol.*, vol. 69, pp. 131–138, Aug. 2021, doi: 10.1016/j.conb.2021.03.003.
5. C. A. Rankin, Q. Sun, and T. C. Gamblin, "Pseudo-phosphorylation of tau at Ser202 and Thr205 affects tau filament formation," *Mol. Brain Res.*, vol. 138, no. 1, pp. 84–93, Jul. 2005, doi: 10.1016/j.molbrainres.2005.04.012.
6. K. Iijima, A. Gatt, and K. Iijima-Ando, "Tau Ser262 phosphorylation is critical for Aβ42-induced tau toxicity in a transgenic Drosophila model of Alzheimer's disease," *Hum. Mol. Genet.*, vol. 19, no. 15, pp. 2947–2957, Aug. 2010, doi: 10.1093/hmg/ddq200.
7. K. SantaCruz et al., "Tau Suppression in a Neurodegenerative Mouse Model Improves Memory Function," *Science*, vol. 309, no. 5733, pp. 476–481, Jul. 2005, doi: 10.1126/science.1113694.
8. P. I. Moreira, C. Carvalho, X. Zhu, M. A. Smith, and G. Perry, "Mitochondrial dysfunction is a trigger of Alzheimer's disease pathophysiology," *Biochim. Biophys. Acta BBA - Mol. Basis Dis.*, vol. 1802, no. 1, pp. 2–10, Jan. 2010, doi: 10.1016/j.bbadis.2009.10.006.
9. J. Liao et al., "Mitochondria in brain diseases: Bridging structural-mechanistic insights into precision-targeted therapies," *Cell Biomater.*, vol. 1, no. 2, Mar. 2025, doi: 10.1016/j.celbio.2025.100016.

 doi:10.20944/preprints202603.0731.v1

10. W. Wang, F. Zhao, X. Ma, G. Perry, and X. Zhu, "Mitochondria dysfunction in the pathogenesis of Alzheimer's disease: recent advances," *Mol. Neurodegener.*, vol. 15, p. 30, May 2020, doi: 10.1186/s13024-020-00376-6.
11. R. S. Balaban, S. Nemoto, and T. Finkel, "Mitochondria, Oxidants, and Aging," *Cell*, vol. 120, no. 4, pp. 483–495, Feb. 2005, doi: 10.1016/j.cell.2005.02.001.
12. H. Murali Mahadevan, A. Hashemiaghdam, G. Ashrafi, and A. B. Harbauer, "Mitochondria in Neuronal Health: From Energy Metabolism to Parkinson's Disease," *Adv. Biol.*, vol. 5, no. 9, p. 2100663, 2021, doi: 10.1002/adbi.202100663.
13. O. Kuryata et al., "Therapeutic potential of 5-aminolevulinic acid in metabolic disorders: Current insights and future directions," *iScience*, vol. 27, no. 12, Dec. 2024, doi: 10.1016/j.isci.2024.111477.
14. L. C. Gardner, S. J. Smith, and T. M. Cox, "Biosynthesis of delta-aminolevulinic acid and the regulation of heme formation by immature erythroid cells in man.," *J. Biol. Chem.*, vol. 266, no. 32, pp. 22010–22018, Nov. 1991, doi: 10.1016/S0021-9258(18)54738-4.
15. H. J. Kim, O. Khalimonchuk, P. M. Smith, and D. R. Winge, "Structure, function, and assembly of heme centers in mitochondrial respiratory complexes," *Biochim. Biophys. Acta BBA - Mol. Cell Res.*, vol. 1823, no. 9, pp. 1604–1616, Sep. 2012, doi: 10.1016/j.bbamcr.2012.04.008.
16. M. Shimura et al., "Effects of 5-aminolevulinic acid and sodium ferrous citrate on fibroblasts from individuals with mitochondrial diseases," *Sci. Rep.*, vol. 9, no. 1, p. 10549, Jul. 2019, doi: 10.1038/s41598-019-46772-x.
17. U. Ota et al., "5-aminolevulinic acid combined with ferrous ion reduces adiposity and improves glucose tolerance in diet-induced obese mice via enhancing mitochondrial function," *BMC Pharmacol. Toxicol.*, vol. 18, no. 1, p. 7, Jan. 2017, doi: 10.1186/s40360-016-0108-3.
18. M. Zhao et al., "5-Aminolevulinic acid with sodium ferrous citrate induces autophagy and protects cardiomyocytes from hypoxia-induced cellular injury through MAPK-Nrf-2-HO-1 signaling cascade," *Biochem. Biophys. Res. Commun.*, vol. 479, no. 4, pp. 663–669, Oct. 2016, doi: 10.1016/j.bbrc.2016.09.156.
19. S. Li et al., "5-Aminolevulinic acid combined with ferrous iron ameliorate ischemia–reperfusion injury in the mouse fatty liver model," *Biochem. Biophys. Res. Commun.*, vol. 470, no. 4, pp. 900–906, Feb. 2016, doi: 10.1016/j.bbrc.2016.01.136.
20. N. Nozawa et al., "5-Aminolevulinic acid and sodium ferrous citrate ameliorate muscle aging and extend healthspan in Drosophila," *FEBS Open Bio*, pp. 295–305, Jan. 2022, doi: 10.1002/2211-5463.13338.
21. N. Nozawa et al., "5-Aminolevulinic acid bypasses mitochondrial complex I deficiency and corrects physiological dysfunctions in Drosophila," *Hum. Mol. Genet.*, vol. 32, no. 16, pp. 2611–2622, Jun. 2023, doi: 10.1093/hmg/ddad092.
22. C. Omori et al., "Facilitation of brain mitochondrial activity by 5-aminolevulinic acid in a mouse model of Alzheimer's disease," *Nutr. Neurosci.*, vol. 20, no. 9, pp. 538–546, Oct. 2017, doi: 10.1080/1028415X.2016.1199114.
23. C. W. Wittmann et al., "Tauopathy in Drosophila: Neurodegeneration Without Neurofibrillary Tangles," *Science*, vol. 293, no. 5530, pp. 711–714, Jul. 2001, doi: 10.1126/science.1062382.
24. G. R. Jackson et al., "Human Wild-Type Tau Interacts with wingless Pathway Components and Produces Neurofibrillary Pathology in Drosophila," *Neuron*, vol. 34, no. 4, pp. 509–519, May 2002, doi: 10.1016/S0896-6273(02)00706-7.
25. I. Nishimura, Y. Yang, and B. Lu, "PAR-1 Kinase Plays an Initiator Role in a Temporally Ordered Phosphorylation Process that Confers Tau Toxicity in *Drosophila*," *Cell*, vol. 116, no. 5, pp. 671–682, Mar. 2004, doi: 10.1016/S0092-8674(04)00170-9.
26. K. Iijima-Ando et al., "Loss of Axonal Mitochondria Promotes Tau-Mediated Neurodegeneration and Alzheimer's Disease–Related Tau Phosphorylation Via PAR-1," *PLoS Genet.*, vol. 8, no. 8, Aug. 2012, doi: 10.1371/journal.pgen.1002918.
27. S. C. Albrecht, A. G. Barata, J. Großhans, A. A. Teleman, and T. P. Dick, "In Vivo Mapping of Hydrogen Peroxide and Oxidized Glutathione Reveals Chemical and Regional Specificity of Redox Homeostasis," *Cell Metab.*, vol. 14, no. 6, pp. 819–829, Dec. 2011, doi: 10.1016/j.cmet.2011.10.010.

 doi:10.20944/preprints202603.0731.v1

28. C. A. Schneider, W. S. Rasband, and K. W. Eliceiri, "NIH Image to ImageJ: 25 years of image analysis," *Nat. Methods*, vol. 9, no. 7, pp. 671–675, Jul. 2012, doi: 10.1038/nmeth.2089.
29. A. C. Costa, S. H. Y. Loh, and L. M. Martins, "Drosophila Trap1 protects against mitochondrial dysfunction in a PINK1/parkin model of Parkinson's disease," *Cell Death Dis.*, vol. 4, no. 1, pp. e467–e467, Jan. 2013, doi: 10.1038/cddis.2012.205.
30. P. M. Quiros, A. Goyal, P. Jha, and J. Auwerx, "Analysis of mtDNA/nDNA Ratio in Mice," *Curr. Protoc. Mouse Biol.*, vol. 7, no. 1, pp. 47–54, 2017, doi: 10.1002/cpmo.21.
31. M. Kohda et al., "A Comprehensive Genomic Analysis Reveals the Genetic Landscape of Mitochondrial Respiratory Chain Complex Deficiencies," *PLoS Genet.*, vol. 12, no. 1, p. e1005679, Jan. 2016, doi: 10.1371/journal.pgen.1005679.
32. G. Pareek, R. E. Thomas, and L. J. Pallanck, "Loss of the Drosophila m-AAA mitochondrial protease paraplegin results in mitochondrial dysfunction, shortened lifespan, and neuronal and muscular degeneration," *Cell Death Dis.*, vol. 9, no. 3, p. 304, Feb. 2018, doi: 10.1038/s41419-018-0365-8.
33. P. Jha, X. Wang, and J. Auwerx, "Analysis of Mitochondrial Respiratory Chain Supercomplexes Using Blue Native Polyacrylamide Gel Electrophoresis (BN-PAGE)," *Curr. Protoc. Mouse Biol.*, vol. 6, no. 1, pp. 1–14, 2016, doi: 10.1002/9780470942390.mo150182.
34. M. Gutscher et al., "Real-time imaging of the intracellular glutathione redox potential," *Nat. Methods*, vol. 5, no. 6, pp. 553–559, Jun. 2008, doi: 10.1038/nmeth.1212.
35. H. Esterbauer, R. J. Schaur, and H. Zollner, "Chemistry and biochemistry of 4-hydroxynonenal, malonaldehyde and related aldehydes," *Free Radic. Biol. Med.*, vol. 11, no. 1, pp. 81–128, Jan. 1991, doi: 10.1016/0891-5849(91)90192-6.
36. K. Iijima-Ando et al., "Loss of Axonal Mitochondria Promotes Tau-Mediated Neurodegeneration and Alzheimer's Disease–Related Tau Phosphorylation Via PAR-1," *PLOS Genet.*, Aug. 2012, doi: 10.1371/journal.pgen.1002918.
37. Y. Castillo-Casaña, C. Arias, and R. Coria, "Tau–Mitochondria Interactions in Neurodegeneration: Mechanisms and Therapeutic Potential," *Cell. Mol. Neurobiol.*, vol. 46, p. 3, Nov. 2025, doi: 10.1007/s10571-025-01634-1.
38. T. E. Tracy et al., "Tau interactome maps synaptic and mitochondrial processes associated with neurodegeneration," *Cell*, vol. 185, no. 4, pp. 712-728.e14, Feb. 2022, doi: 10.1016/j.cell.2021.12.041.
39. E. Maranzana, G. Barbero, A. I. Falasca, G. Lenaz, and M. L. Genova, "Mitochondrial Respiratory Supercomplex Association Limits Production of Reactive Oxygen Species from Complex I," *Antioxid. Redox Signal.*, vol. 19, no. 13, pp. 1469–1480, Nov. 2013, doi: 10.1089/ars.2012.4845.
40. M. L. Genova and G. Lenaz, "Functional role of mitochondrial respiratory supercomplexes," *Biochim. Biophys. Acta BBA - Bioenerg.*, vol. 1837, no. 4, pp. 427–443, Apr. 2014, doi: 10.1016/j.bbabio.2013.11.002.
41. S. Shimada et al., "A unique respiratory adaptation in *Drosophila* independent of supercomplex formation," *Biochim. Biophys. Acta BBA - Bioenerg.*, vol. 1859, no. 2, pp. 154–163, Feb. 2018, doi: 10.1016/j.bbabio.2017.11.007.
42. F. Bartolome, E. Carro, and C. Alquezar, "Oxidative Stress in Tauopathies: From Cause to Therapy," *Antioxidants*, vol. 11, no. 8, p. 1421, Jul. 2022, doi: 10.3390/antiox11081421.
43. M. L. Steinhilb, D. Dias-Santagata, T. A. Fulga, D. L. Felch, and M. B. Feany, "Tau Phosphorylation Sites Work in Concert to Promote Neurotoxicity In Vivo," *Mol. Biol. Cell*, vol. 18, no. 12, Oct. 2007, doi: 10.1091/mbc.e07-04-0327.
44. S. Chatterjee, T.-K. Sang, G. M. Lawless, and G. R. Jackson, "Dissociation of tau toxicity and phosphorylation: role of GSK-3β, MARK and Cdk5 in a Drosophila model," *Hum. Mol. Genet.*, vol. 18, no. 1, pp. 164–177, Jan. 2009, doi: 10.1093/hmg/ddn326.
45. S. Mondragón-Rodríguez, G. Perry, X. Zhu, P. I. Moreira, M. C. Acevedo-Aquino, and S. Williams, "Phosphorylation of Tau Protein as the Link between Oxidative Stress, Mitochondrial Dysfunction, and Connectivity Failure: Implications for Alzheimer's Disease," *Oxid. Med. Cell. Longev.*, pp. 1–6, Jul. 2013, doi: 10.1155/2013/940603.

 doi:10.20944/preprints202603.0731.v1

46. J. Biernat, N. Gustke, G. Drewes, E.-. Mandelkow, and E. Mandelkow, "Phosphorylation of Ser262 strongly reduces binding of tau to microtubules: Distinction between PHF-like immunoreactivity and microtubule binding," *Neuron*, vol. 11, no. 1, pp. 153–163, Jul. 1993, doi: 10.1016/0896-6273(93)90279-Z.
47. N. Donison, J. Palik, K. Volkening, and M. J. Strong, "Cellular and molecular mechanisms of pathological tau phosphorylation in traumatic brain injury: implications for chronic traumatic encephalopathy," *Mol. Neurodegener.*, vol. 20, no. 1, p. 56, May 2025, doi: 10.1186/s13024-025-00842-z.
48. R. C. Rabinovitch et al., "AMPK Maintains Cellular Metabolic Homeostasis through Regulation of Mitochondrial Reactive Oxygen Species," *Cell Rep.*, vol. 21, no. 1, pp. 1–9, Oct. 2017, doi: 10.1016/j.celrep.2017.09.026.